EUROPEAN SYNCHROTRON RADIATION FACILITY

A

	Experiment title: **Study of internalization, distribution and Ce^{3+}/Ce^{4+} equilibrium in cells exposed to Ceria nanoparticles with antioxidant activity by micro-XANES spectroscopy**	**Experiment number**: CH-4716
Beamline: ID21	**Date of experiment**: from: 20/04/2016 to: 23/04/2016	**Date of report**: 29/08/2016
Shifts: 9	**Local contact(s)**: Hiram Castillo-michel, Ana Elena Pradas	*Received at ESRF:*

Names and affiliations of applicants (* indicates experimentalists):

Paolo Ghigna (Università di Pavia, Italy)*

Patrizia Sommi (Università di Pavia, Italy)*

Umberto Anselmi Tamburini (Università di Pavia, Italy)*

Ilenia Tredici (Università di Pavia, Italy)*

Daniela Ferraro (Università di Pavia, Italy)*

Vittorio Ricci (Università di Pavia, Italy)

Report:

Background Reactive oxygen species (ROS) and reactive nitrogen species (RNS) derive from free radicals originated by metabolic reactions. The extent and the severity of the damage exerted by ROS, /RNS is largely dependent on the cell ability in neutralizing these reactive species through physiological free radical scavengers, such as superoxide dismutase, catalase and glutathione peroxidase. When free radicals concentrations exceed the antioxidant capacity of the cells, the normal cell physiology can be altered causing a general suffering condition known as “oxidative stress”. Oxidative stress and generation of free radicals have been associated with some neurodegenerative conditions, like aging, Alzheimer’s and Parkinson’s diseases. It has also been found that high level of ROS can alter the immune response, causing chronic inflammation and immunological disorders, and produce DNA damage, activating the oncogenes and inactivating the suppressor genes. CeO_2 nanoparticles (CNPs) are at the moment actively investigated as promising agents in the therapy of a number of pathologies involving free radicals or oxidative stress.

Aim A description of the mechanism of action of CNPs in human cells is still missing. The present study aims at bridging this gap, by investigating, in human cells, the modification of Ce(III)/Ce(IV) ratio following cell-internalization and its dependence from the intra-cellular localization.

Experimental description.

HeLa cells were grown on Si_3N_4 membranes and treated with CNP as described above. At the end of incubation, samples were freeze-dryed using the immersion freezing procedure with liquid nitrogen (LN_2) container surrounding the Liquid Propane (LP) as secondary cryogen. Si_3N_4 membranes are first blotted on filter paper then the samples are immersed face up in LP. Each membrane was sealed in vials under LN_2-vapors to avoid ice-crystals formation, then maintained at -80°C. For the X-ray synchrotron analysis, the

samples were mounted in the pre cooled sample holder under LN_2-vapors and then immediately inserted into the cryostat. The entire transfer process took less than 2 minutes. Synchrotron radiation µXRF and Ce L_{III}-edge µXANES measurements were performed using the scanning X-ray microscope of beamline ID21 at the European Synchrotron Radiation Facility (ESRF, Grenoble, France). The beamline is equipped with a cryo-stage which is passively cooled by a liquid LN_2 dewar keeping the sample stable at -170 ±5°C. The photon flux was 5.7×10^{10} ph s^{-1} at 5.8 keV with a beam size of 1.0 x 0.5 µm² (HxV). The µXRF maps were acquired with an incoming energy of 5.8 keV with 0.5 μm^2 steps and integration time of 100-150 ms. The µXRF acquisition was done in hyperspectral mode where the XRF spectrum for each pixel in the image is registered, all maps were then fitted using PyMCA to obtain intensity distribution of elements. The µXANES spectra were acquired in fluorescence mapping mode by scanning the beam with a $0.6 \times 0.6 \mu m^2$ step size and a 100ms dwell time per pixel with 5eV energy steps in the region from 5.68 keV to 5.72 keV, 0.5eV from 5.72 keV to 5.77 keV, and 2eV from 5.77 keV to 5.84 keV. This resulted in a total of 129 images recorded using a region of interest selective for Ce L3M4 and L3M5 emission lines, corrected for detector dead time and normalized by I_0. The stack of images were aligned using elastix and saved to an hdf5 file containing intensities and the energy values for each map to be processed using PyMCA for XANES spectra extraction.

Results Fig. 6 shows the in situ XANES analysis of oxidation state of Ce. In particular, panel A shows a representative single cell color-coded map of K, which indicates the cell position, and the corresponding map of Ce distribution. It is well apparent tha Ce is mainly present in well-defined hot spots (red), from where it is visible a clear concentration gradients (from yellow to green); the rectangular area is further enlarged to magnify the areas of interest (A). We then extracted the XANES spectra from the 1, 2 and 3 regions in the cell showing different concentrations of Ce. Spectrum 1 was taken in the "hot spot" areas (red); spectrum 2 in the overall green areas (green); and spectrum 3 in the rest of the overall area (azure).

The acquired spectra are can then be compared with those of CeO_2 and $Ce(NO_3)_3 \bullet 6H_2O$ that are used as standard for Ce(IV) and Ce(III), respectively. Remarkably, significant differences can be observed between these spectra. Spectrum 1, in fact, is very similar to that of bulk CeO_2. From this observation we can conclude that the CNP located in the hot spots presents Ce atoms in the Ce(IV) oxidation state. An increase in the spectral intensity at ca. 5723 eV is well apparent in spectrum 2 and is even more evident in spectrum 3. In this same energy region Ce(III) presents an intense white line. It follows that in the region of the cell away from the hot spots an higher content of Ce(III) can be observed. To quantify the Ce(III)/Ce(IV) relative amount, 2 and 3 spectra have been fitted as linear combinations of the spectrum 1 (used as reference for Ce(IV)), and the spectrum of $Ce(NO_3)_3 \cdot 6H_2O$. These fittings were performed using the derivatives in order to evidence better the shift in energy of the absorption edges. The best fit has been obtained considering concentrations of Ce(III) of 12% for spectrum 2 and 17% for spectrum 3.

Conclusion With this experiment we have demonstrated that the Ce(III)/Ce(IV) redox couple plays an effective role in the internalisation of CeO_2 nanoparticles in HeLa cells. This in turn strongly support the idea that the Ce(III)/Ce(IV) redox couple is at the basis of the action mechanisms of CeO_2 in decreasing oxidative stress.

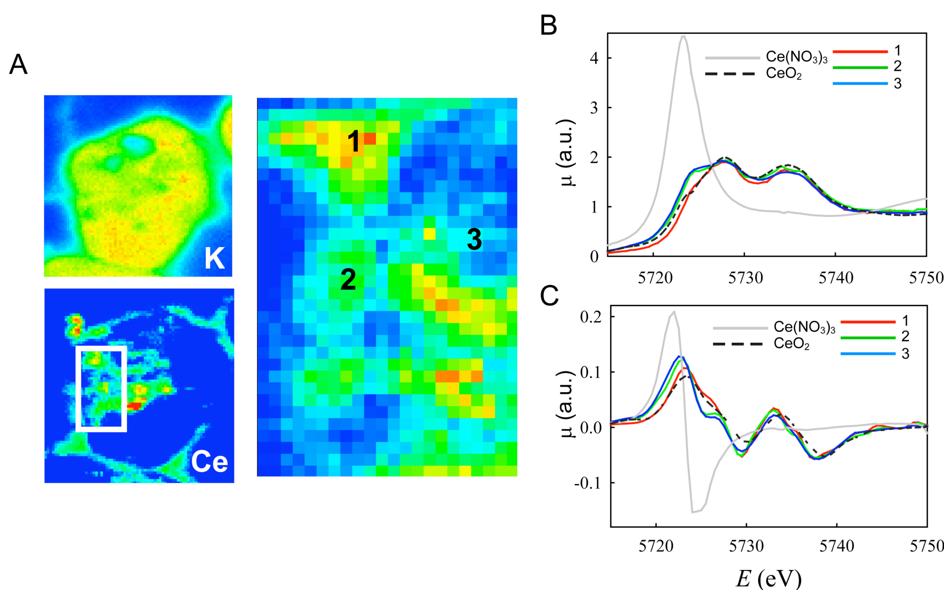

Fig. 1